ELSEVIER

Journal of Nuclear Materials 283–287 (2000) 1346–1350

journal of nuclear materials

www.elsevier.nl/locate/jnucmat

Copper corrosion and activation in water cooling loops under fusion irradiation conditions

P.J. Karditsas [a,*], S.M. Ali [b], D. Wan [c]

[a] *EURATOM/UKAEA Fusion Association, Culham Science Centre, Abingdon, Oxon, OX14 3DB, UK*
[b] *NNC Ltd., Warrington Rd, Risley, Cheshire WA3 6BZ, UK*
[c] *BSc Engineering Physics, Sheffield Hallam University, Sheffield S1 1WB, UK*

Abstract

Copper alloys have recently been proposed in the design of the International Thermonuclear Experimental Reactor (ITER), Spherical Tokamak (ST) power plants (ARIES ST, Culham ST), and have been used in the construction of the central column of experimental machines like MAST (UKAEA) and NSTX (PPPL). The activation–corrosion code transport of activation (TRACT) is used to predict corrosion, transport behaviour, and activity in the central column-cooling loop of the ST power plant. A 2 yr irradiation of the central column results in coolant activity due to the ^{66}Cu, ^{62}Cu, ^{16}N and ^{64}Cu nuclides. After power down, activity is dominated by ^{64}Cu, but after a few days it is due to the long-lived nuclides. The solubility and radiolysis models developed here can be used to predict corrosion release rates and the necessary water chemistry conditions to minimise activated products in cooling loops of fusion experimental machines and future power plants. © 2000 UKAEA. Published by Elsevier Science B.V. All rights reserved.

1. Introduction

Activation products on or near the primary cooling loop pipe inner surfaces of power plants are mobilised and enter the coolant. Once entrained or dissolved they are transported around the cooling loop, with a fraction of the activity captured in filters and ion exchange resins and the remaining fraction deposited onto surfaces in other parts of the cooling loop. Plant workers inspecting or maintaining cooling circuit equipment may thus experience radiation exposure. Also of interest is the potential for release of radionuclides from the cooling circuits following some loop accident.

Theoretical and experimental work has been performed, and a number of computational models have been developed, to describe and predict activation product transport and deposition in fission power plants [1,2]. In recent years, some of these codes and models have been modified to examine the activation product behaviour in water-cooled fusion power plants [3,4]. These codes and models were specific to stainless steel surfaces and could not predict conditions for copper pipework. This paper presents a copper corrosion model and subsequent results obtained for the activation and corrosion of the copper alloy central column of a Spherical Tokamak (Culham ST) power plant.

2. Copper corrosion model

A comprehensive overview of the domains of thermodynamic stability of various copper compounds in water can be obtained from the potential–pH diagram. Simplified diagrams for the copper–water system at 298 and 562 K have been given by Cubicciotti [5] and more detailed diagrams are available in [6]. At ordinary temperatures, copper will not corrode in deaerated water free from oxidizing agents, because the electrode potential of Cu/Cu^{++} is more noble than the H_2/H^+ hydrogen electrode. In aerated oxidising conditions, copper will dissolve in acid solutions and oxidise in neutral and alkaline solutions. At low temperatures and

---

[*] Corresponding author. Tel.: +44-1235 464 277; fax: +44-1235 463 435.

E-mail address: panos.karditsas@ukaea.org.uk (P.J. Karditsas).

0022-3115/00/$ - see front matter © 2000 UKAEA. Published by Elsevier Science B.V. All rights reserved.
PII: S0022-3115(00)00122-7

mildly oxidising conditions, copper dissolves as Cu^{++} ions in acid solutions and oxidises to Cu_2O in neutral and alkaline solutions. When the potential is further increased, Cu_2O will be converted to CuO and/or $Cu(OH)_2$ in neutral and weak alkaline solutions. At high temperatures, copper dissolves as Cu^+ ions, which can then oxidise to Cu^{++} ions at the higher potentials in acid solutions. In weak alkaline solutions, copper is oxidised to Cu_2O, but converts to CuO at higher potentials.

In general, water radiolysis produces oxidising conditions (due to the formation of O_2, H_2O_2, etc.) which raise the oxidation potential and consequently change the thermodynamic equilibrium concentrations of the dissolving metal ions. A potential–pH diagram of the copper–water system in the presence of H_2O_2 is given in [7]. A literature search on the aqueous corrosion of copper under fusion irradiation conditions has shown the sparsity of publications in this field [8]. The available literature mainly relates to copper cannisters for use in nuclear waste disposal [9,10].

Following the approach in [5], a set of reactions is used to describe the copper–water system:

(a) $CuO + 2H^+ = Cu^{++} + H_2O$,
(b) $2FeCuO_2 + 4H^+ = 2Cu^{++} + Fe_2O_3 + H_2O + H_2$,
(c) $Cu_2O + 4H^+ = 2Cu^{++} + H_2O$,
(d) $Cu + 2H^+ = Cu^{++} + H_2$,
(e) $CuO + \frac{1}{2}H_2 + H^+ = Cu^+ + H_2O$,
(f) $2FeCuO_2 + 2H^+ = 2Cu^+ + Fe_2O_3 + H_2O$,
(g) $Cu + H^+ = Cu^+ + \frac{1}{2}H_2$,
(h) $Cu_2O + 2H^+ = 2Cu^+ + H_2O$,
(i) $Cu + H_2O_2 = Cu^+ + OH + OH^-$.

The reactions (a)–(i) are used to produce a model that allows calculation of copper solubility under various water conditions. The individual contributions to the total solubility are dependent on the hydrogen ion concentration, the hydrogen partial pressure, the reaction equilibrium constants, and the water ionisation constant [11]. The most widely used mechanism in the nuclear industry to control free radicals that cause oxidation of metal surfaces, and suppress radiolysis, is injection of hydrogen into the cooling loop. Calculations have shown [12] a $\sim$1000 times increase in oxygen partial pressure due to irradiation at PWR core operating conditions with a similar reduction in hydrogen partial pressure (equilibrium conditions) [13]. A decrease in hydrogen partial pressure affects the solubility of copper corrosion products and leads to increased copper release by corrosion in the exposed to irradiation (in-flux) regions. The enhancement of copper corrosion due to radiolysis has not been investigated in detail, although there is evidence of increased copper corrosion in the presence of gamma radiation in particle accelerator cooling water systems [14].

Parameters that affect water radiolysis are: the nature of the primary energy (fast neutrons, electrons, gamma rays), the rate of absorption of energy (radiation intensity, linear energy transfer rate (LET)), and the water chemistry (oxidant or reductant concentration). It is proposed, until a detailed model is derived, to approximate concentrations of injected hydrogen C_{H_2} (ml/kg) for suppression of radiolysis in fusion power plant cooling channels using an empirical equation, based on experiments at the NRU reactor [15]:

$$C_{H_2} = 0.1054\, P^{0.5}\left(\frac{n}{\gamma}\right)(\mathrm{SR}) \tag{1}$$

with P (W/g) the heat deposition, n/γ the neutron to gamma ratio, SR the stripping ratio, and the constant (0.1054) relating to the NRU, U-2 loop experiment. It should be noted that a mean LET of $\leqslant 4$ eV/nm associated with 14 MeV fusion neutrons is lower than the mean LET of 40 eV/nm generally assigned to the fission neutrons. Therefore, the higher energy neutrons from fusion devices would not necessarily give rise to greater radiolysis of coolant water, instead a reduction is possible. On this basis, it can be assumed that Eq. (1) may give conservative results. Assuming that solubility of the most stable species in solution is at a minimum, the following rule can be used to calculate the system solubility C_T (mol/kg):

$$C_T = \min\left\{\underbrace{(C_a + C_e)}_{\mathrm{CuO}}\underbrace{(C_b + C_f)}_{\mathrm{FeCuO_2}}\underbrace{(C_c + C_h)}_{\mathrm{Cu_2O}}\underbrace{(C_d + C_g + C_i)}_{\mathrm{Cu}}\right\} \tag{2}$$

C_a–C_i being the equilibrium constants with the reactions (a)–(i).

The corrosion rate of copper from [16] is in the range 37–188 mdm, with mdm denoting milligram per decimetre square per month (1 mdm $= 3.858 \times 10^{-11}$ kg/m^2 s). Other experimental studies [17] give values of copper corrosion in range 45–75 mdm under different conditions. The corrosion rate for copper is assumed to be variable with time [11], and an expression that reliably fits the data is

$$G_C = 2.0 \times 10^{-7} t^{-0.217}\ \mathrm{kg/m^2\,s} \tag{3}$$

with the time t in seconds. This results in an average corrosion rate of $\sim$130 mdm in a period of 2 yr. The corrosion rate of stainless steel [18] is

$$G_C = 2.632 \times 10^{-7} t^{-0.6}\ \mathrm{kg/m^2\,s} \tag{4}$$

3. The ST central column: data calculations

The code TRACT [19] is used to calculate the corrosion product mass transfer and activity content of cooling loops. Here, coolant and pipe surface atomic and activity concentrations are calculated for the central column-cooling loop of an ST.

The cooling channel wall material is a copper alloy (Glidcop) and the out-of-flux pipework material is austenitic stainless steel SS316. The assumed composition (wt%) of the materials is: copper alloy (in-flux, Cu – 99.5, Al – 0.25, O – 0.25), and 316SS (out-of-flux, Fe – 67.0, Cr – 18.0, Mn – 2.00, Ni – 12.95, Co – 0.05). A detailed description of the cooling loop can be found in [20]. The calculations assume the loop has a total length of 134 m, pressure 0.2 MPa, temperature 30°C (inlet) and 50°C (outlet), and mass flow rate 3836 kg/s. The clean-up rate is assumed to be 0.25% of the main flow rate, i.e., 9.59 kg/s are diverted to the filters and resins at all times, with an assumed collection efficiency of 50%. The central column is cooled through 2180 evenly spread channels of 15 mm diameter and 18 m in length (they occupy 15% of the cross-sectional area). The water flow velocity is ∼10 m/s and the cooling loop pipe sizes are chosen, accordingly, to match this value. The mass transfer coefficients range for solubles between 0.6 and 2.16 μm/s, and for insolubles between 4.41 and 21.2 μm/s.

Since water flows both through copper alloys (in-flux) and stainless steel (out-of-flux), it is desirable to balance the solubility in the loop, to avoid large deposition in the out-of-flux regions. Fig. 1 shows the variation of copper alloy and steel solubility at 30°C and 50°C with added hydrogen. The H_2 needed to balance the solubilities is $\sim 1.0 \times 10^{-14}$ ml/kg. Using Eq. (1), the injected hydrogen required to supress radiolysis for this loop is 0.088 ml/kg, see Fig. 1. The resulting water loop chemistry is very different for the balanced in-flux and out-of-flux solubility cases. The copper solubility is in the range $7.8–140.0 \times 10^{-15}$ mol/kg and that of stainless steel in the range $1.84–2.01 \times 10^{-6}$ mol/kg.

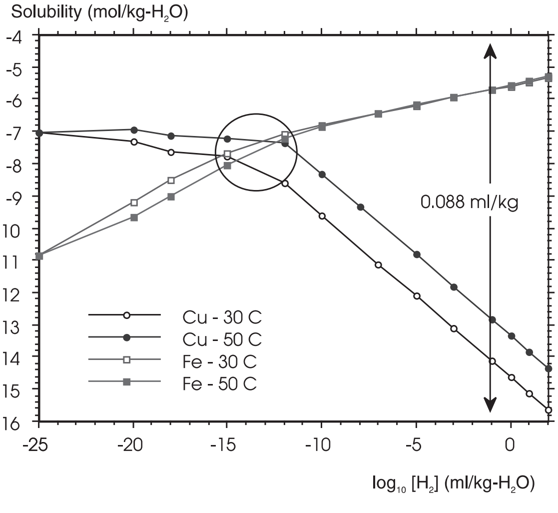

Fig. 1. Copper alloy and stainless steel solubility variation with injected hydrogen concentration.

Steady irradiation of the components is assumed for a period of 2 yr. The neutron spectrum variation along the length of the column was determined from Monte Carlo calculations [21] using the general purpose coupled neutron/photon transport code MCNP-4a. The irradiation flux values range between 5.58×10^{13} and 1.785×10^{18} nm^2/s. A preliminary activation investigation led to the inclusion of 19 species to be treated (in order of increasing half life): ^{28}Al, ^{66}Cu, ^{62}Cu, ^{56}Mn, ^{58m}Co, ^{64}Cu, ^{57}Ni, ^{51}Cr, ^{59}Fe, ^{57}Co, ^{54}Mn, ^{58}Co, ^{55}Fe, ^{60}Co, ^{60m}Co, ^{63}Ni, ^{59}Ni, and the gases ^{3}H and ^{16}N.

The gas production rates in the solid and coolant are determined from a series of calculations using the code FISPACT-99 [22]. Calculated values for the in-flux regions range for tritium between $3.35 \times 10^{9}–1.07 \times 10^{14}$ at./m^3 s (copper) and $3.02 \times 10^{4}–9.67 \times 10^{8}$ at./m^3 s (coolant), and for ^{16}N between $2.06 \times 10^{9}–6.59 \times 10^{13}$ at./m^3 s (copper) and $8.42 \times 10^{8}–2.69 \times 10^{13}$ at./m^3 s (coolant).

Results show that initially, material is released into the loop from a large proportion of the in- and out-of-flux surface area, but after a few hours conditions are such that the release of material into the loop is entirely from the out-of-flux region. This is predominantly the effect of the ∼7–8 orders of magnitude higher solubility of the out-of-flux region, a result reflecting the water chemistry to suppress radiolysis. Of the two gases investigated, ^{3}H tends to diffuse to the surrounding pipework whereas ^{16}N tends to stay in the coolant. The decrease of ^{16}N concentration in the out-of-flux region (20–134 m) is entirely due to its fast decay. With a half life of ∼7 s, ^{16}N is expected to decay approximately by a factor $\exp(\lambda t)$, with $t = (114\text{ m})/(10\text{ m/s}) = 11.4$ s, or to 0.26 of its central column outlet value of 1.5×10^{13} at./m^3, i.e., $\sim 3.9 + 12$ at./m^3. This is the value calculated by TRACT. The 743 days tritium concentration of 1.8×10^{12} at./m^3 shows no significant variation around the cooling loop.

The thicknesses of the corroded (or 'oxide') layers are calculated to be 37.1 μm (in-flux) and 0.106 μm (out-of-flux). The code for a 2 yr period predicts negligible in-flux average release rate and 6.92×10^{-12} kg/m^2 s for

Table 1
Mass inventory (2 yr operation)

	In-flux	Out-of-flux
Releases (g)	∼0.0	1650.0
Deposits (g)	1017.0	456.0
Coolant solubles (mg)	0.11	1.09
Coolant crud (mg)	2.62	20.60
Filters/resins (g)	177.0	

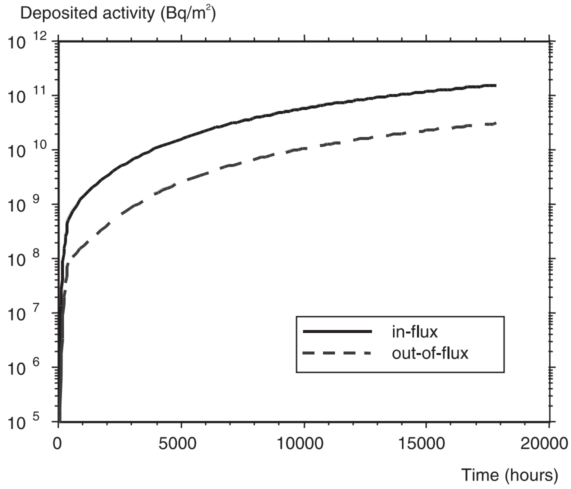

Fig. 2. Variation of deposited activity with time.

Table 2
Total activity inventory (2 yr operation)

	In-flux	Out-of-flux
Oxide layer (Bq/m^2)	1.74×10^{13}	1.42×10^{4}
Deposits (Bq/m^2)	1.67×10^{11}	3.28×10^{10}
Coolant solubles (Bq/m^3)	1.43×10^{13}	1.36×10^{13}
Coolant crud (Bq/m^3)	4.48×10^{11}	4.48×10^{11}
Resins/solubles (Bq)	1.16×10^{16}	
Filters/crud (Bq)	2.06×10^{14}	

out-of-flux, which corresponds to a 50% loss of thickness of the out-of-flux corroded layer. The results show that the material mobilised to the coolant is entirely due to releases in the out-of-flux part of the loop. Of the total mass released 89% deposits (62% in-flux, 38% out-of-flux) and 11% is cleaned by the filters and resins. The cooling loop water chemistry and solubility results in more mass deposited in the in-flux region. A summary of the mass inventory in the loop is given in Table 1.

The loop coolant activity is entirely due to the soluble active nuclides, with 90% contributed by the short lived nuclides ^{66}Cu, ^{62}Cu, ^{16}N, and 10% by the longer-lived ^{64}Cu. The corrosion and deposited layer activity, Fig. 2, is dominated ($\geqslant$90%) by the ^{64}Cu nuclide. Activity a few days after power down is entirely due to the long-lived nuclides and is lower by 3–4 orders of magnitude depending on location. Major contributors are ^{60}Co, ^{60m}Co, ^{63}Ni and to a lesser extend ^{51}Cr. A summary of total coolant and surface activity is given in Table 2.

It can be concluded that this analysis and the solubility and radiolysis models developed can be used to predict corrosion release rates and the necessary water chemistry conditions to minimise activated products in cooling loops of fusion experimental machines and future power plants.

Acknowledgements

This work was jointly funded by the UK DTI and EURATOM.

References

[1] T. Chandrasekan et al., Calculation of releases of radioactive material in gaseous and liquid effluents from pressurised water reactors (PWR-GALE code), NUREG-0017, US Nuclear Regulatory Commission, Office of Standards Development, 1976.

[2] P. Beslu, PACTOLE: a calculational code for predicting corrosion product behaviour and activation in PWR primary coolant systems. CEA Cadarache Report, SCOC/LCC/90-096, 1990.

[3] C.C. Baker et al., STARFIRE – a commercial tokamak fusion power plant study, Argonne National Lab. Report, ANL/FPP-80-1, Appendix G, 1980.

[4] K.R. Smith, C.B.A. Forty, Estimation of the radioactive content of the primary circuit of a water-cooled fusion reactor and the annual liquid effluent source term, AEA FUS 108 (1991).

[5] D. Cubicciotti, Pourbaix Diagrams for Mixed Metal Oxides, Chemistry of Copper in BWR Water, Corrosion, NACE, 44 (12) (1988) 875.

[6] C.M. Chen, K. Aral, J. Theus, Computer calculated potential pH diagrams to 300C, vol. 2, EPRI NP 3137 (1983).

[7] K.J.A. Kundig, D.T. Peters, Proc. Waste Management (1991) 677.

[8] K.A. Nikishina, N.G. Ziverding, Effect of ionizing radiation on the corrosion and mechanical behaviour of dispersion-hardened copper alloys, NEA Specialist meeting on erosion and corrosion of nuclear power plant materials, Kiev, 1994, p. 87.

[9] F. King, C.D. Litke, Corrosion of copper under Canadian nuclear fuel waste disposal conditions, in: Proceedings of Workshop on Corrosion of Nuclear Fuel Waste Containers, Winnipeg, Canada, 1990, p. 119.

[10] F. King, Y. Tang, M.J. Quinn, C.D. Litke, The effect of dissolved oxygen concentration and mass-transport conditions on the dissolution behaviour of copper nuclear waste containers, Paper 424, NACE, Corrosion 95, 1995.

[11] S.M. Ali, Final Report on the Investigation of the Copper–Water System, NNC Report C5590/TR/001, Issue V02, February 1998.

[12] T.E. Rummery, D.D. Macdonald, J. Nucl. Mater. 55 (1975) 23.

[13] G.N. Walton, Underlying mechanism in the water chemistry of nuclear system, in: International Conference on Water Chemistry of Nuclear Reactor System, BNES, London, 1977.

[14] H. Scholer, H. Euteneuer, Corrosion of copper by deionized cooling water, European Particle Acceleration Conference (EPAC-l) Rome, Italy, 1988, p. 1067.

[15] D.R. McCracken, Coolant radiolysis and boiling in water-cooled reactors, EPRI-TR-100789, Electric Power Research Institute, 1992.

[16] F.L. La Que, H.R. Copson, American Chemical Society Monograph Series, 2nd Ed., Reinhold, New York, 1963.
[17] S.A. Olszowka, M.A. Manning, A. Barkatt, Copper dissolution and hydrogen peroxide formation in aqueous media, Corrosion, NACE, 48(S) (1992) 411.
[18] V. Belous et al., J. Nucl. Mater. 258–263 (1998) 351.
[19] P.J. Karditsas, Fus. Eng. Design 45 (1999) 169.
[20] G.M. Voss, Toroidal field coil design for the ST power plant, in: Proceedings of the Sixth IAEA Technical Committee Meeting and Workshop, IAEA, Culham, UK, 24–27 March 1998.
[21] P.J. Karditsas, J.E.M. Edwards, Blanket and first wall conceptual design issues of the Spherical Tokamak power plant, in: Proceedings of the Sixth IAEA Technical Committee Meeting and Workshop, IAEA, Culham, UK, 24–27 March 1998.
[22] R.A. Forrest, J-Ch. Sublet, FISPACT-99: User manual, UKAEA FUS 407, Euratom/UKAEA Fusion Association, Culham Science Centre, Abingdon, UK, 1998.